Figure S3. SH-SY5Y neuronal cells were untreated (Control) or treated with 0.25 mM ARS for 0.5 h, and then analyzed by fluorescence *in situ* hybridization, as indicated.

References

Anderson P. and Kedersha N. (2009) RNA granules: post-transcriptional and epigenetic modulators of gene expression. *Nat. Rev. Mol. Cell Biol.* **10**, 430–436.

Arai T., Hasegawa M., Akiyama H. *et al.* (2006) TDP-43 is a component of ubiquitin-positive tau-negative inclusions in frontotemporal lobar degeneration and amyotrophic lateral sclerosis. *Biochem. Biophys. Res. Commun.* **351**, 602–611.

Arimoto K., Fukuda H., Imajoh-Ohmi S., Saito H. and Takekawa M. (2008) Formation of stress granules inhibits apoptosis by suppressing stress-responsive MAPK pathways. *Nat. Cell Biol.* **10**, 1324–1332.

Ayala V., Granado-Serrano A. B., Cacabelos D. *et al.* (2011) Cell stress induces TDP-43 pathological changes associated with ERK1/2 dysfunction: implications in ALS. *Acta Neuropathol.* **122**, 259–270.

Bruijn L. I., Miller T. M. and Cleveland D. W. (2004) Unraveling the mechanisms involved in motor neuron degeneration in ALS. *Annu. Rev. Neurosci.* **27**, 723–749.

Buchan J. R. and Parker R. (2009) Eukaryotic stress granules: the ins and outs of translation. *Mol. Cell* **36**, 932–941.

Ceman S., O'Donnell W. T., Reed M., Patton S., Pohl J. and Warren S. T. (2003) Phosphorylation influences the translation state of FMRP-associated polyribosomes. *Hum. Mol. Genet.* **12**, 3295–3305.

Cleveland D. W. and Rothstein J. D. (2001) From Charcot to Lou Gehrig: deciphering selective motor neuron death in ALS. *Nat. Rev. Neurosci.* **2**, 806–819.

Cohen T. J., Hwang A. W., Unger T., Trojanowski J. Q. and Lee V. M. (2011) Redox signalling directly regulates TDP-43 via cysteine oxidation and disulphide cross-linking. *EMBO J.* **31**, 1241–1252.

Colombrita C., Zennaro E., Fallini C., Weber M., Sommacal A., Buratti E., Silani V. and Ratti A. (2009) TDP-43 is recruited to stress granules in conditions of oxidative insult. *J. Neurochem.* **111**, 1051–1061.

Cuesta R., Laroia G. and Schneider R. J. (2000) Chaperone hsp27 inhibits translation during heat shock by binding eIF4G and facilitating dissociation of cap-initiation complexes. *Genes Dev.* **14**, 1460–1470.

Dewey C. M., Cenik B., Sephton C. F., Dries D. R., Mayer P. III, Good S. K., Johnson B. A., Herz J. and Yu G. (2011) TDP-43 is directed to stress granules by sorbitol, a novel physiological osmotic and oxidative stressor. *Mol. Cell. Biol.* **31**, 1098–1108.

Feng Y., Absher D., Eberhart D. E., Brown V., Malter H. E. and Warren S. T. (1997) FMRP associates with polyribosomes as an mRNP, and the I304N mutation of severe fragile X syndrome abolishes this association. *Mol. Cell* **1**, 109–118.

Gauthier D. and Ven Murthy M. R. (1987) Efficacy of RNase inhibitors during brain polysome isolation. *Neurochem. Res.* **12**, 335–339.

Gilks N., Kedersha N., Ayodele M., Shen L., Stoecklin G., Dember L. M. and Anderson P. (2004) Stress granule assembly is mediated by prion-like aggregation of TIA-1. *Mol. Biol. Cell* **15**, 5383–5398.

Gomes M. P., Cordeiro Y. and Silva J. L. (2008) The peculiar interaction between mammalian prion protein and RNA. *Prion* **2**, 64–66.

Higashi S., Iseki E., Minegishi M., Togo T., Kabuta T. and Wada K. (2010) GIGYF2 is present in endosomal compartments in the mammalian brains and enhances IGF-1-induced ERK1/2 activation. *J. Neurochem.* **115**, 423–437.

Holcik M. and Sonenberg N. (2005) Translational control in stress and apoptosis. *Nat. Rev. Mol. Cell Biol.* **6**, 318–327.

Iguchi Y., Katsuno M., Takagi S., Ishigaki S., Niwa J., Hasegawa M., Tanaka F. and Sobue G. (2012) Oxidative stress induced by glutathione depletion reproduces pathological modifications of TDP-43 linked to TDP-43 proteinopathies. *Neurobiol. Dis.* **45**, 862–870.

Kabashi E., Valdmanis P. N., Dion P. *et al.* (2008) TARDBP mutations in individuals with sporadic and familial amyotrophic lateral sclerosis. *Nat. Genet.* **40**, 572–574.

Kawai T., Fan J., Mazan-Mamczarz K. and Gorospe M. (2004) Global mRNA stabilization preferentially linked to translational repression during the endoplasmic reticulum stress response. *Mol. Cell. Biol.* **24**, 6773–6787.

Kedersha N., Cho M. R., Li W., Yacono P. W., Chen S., Gilks N., Golan D. E. and Anderson P. (2000) Dynamic shuttling of TIA-1 accompanies the recruitment of mRNA to mammalian stress granules. *J. Cell Biol.* **151**, 1257–1268.

Kedersha N., Chen S., Gilks N., Li W., Miller I. J., Stahl J. and Anderson P. (2002) Evidence that ternary complex (eIF2-GTP-tRNA(i)(Met))-deficient preinitiation complexes are core constituents of mammalian stress granules. *Mol. Biol. Cell* **13**, 195–210.

Kedersha N., Stoecklin G., Ayodele M. *et al.* (2005) Stress granules and processing bodies are dynamically linked sites of mRNP remodeling. *J. Cell Biol.* **169**, 871–884.

Kim W. J., Back S. H., Kim V., Ryu I. and Jang S. K. (2005) Sequestration of TRAF2 into stress granules interrupts tumor necrosis factor signaling under stress conditions. *Mol. Cell. Biol.* **25**, 2450–2462.

Kwiatkowski T. J. Jr, Bosco D. A., Leclerc A. L. *et al.* (2009) Mutations in the FUS/TLS gene on chromosome 16 cause familial amyotrophic lateral sclerosis. *Science* **323**, 1205–1208.

Liu-Yesucevitz L., Bilgutay A., Zhang Y. J. *et al.* (2010) Tar DNA binding protein-43 (TDP-43) associates with stress granules: analysis of cultured cells and pathological brain tissue. *PLoS ONE* **5**, e13250.

Lu L., Wang S., Zheng L. *et al.* (2009) Amyotrophic lateral sclerosis-linked mutant SOD1 sequesters Hu antigen R (HuR) and TIA-1-related protein (TIAR): implications for impaired post-transcriptional regulation of vascular endothelial growth factor. *J. Biol. Chem.* **284**, 33989–33998.

McDonald K. K., Aulas A., Destroismaisons L., Pickles S., Beleac E., Camu W., Rouleau G. A. and Vande Velde C. (2011) TAR DNA-binding protein 43 (TDP-43) regulates stress granule dynamics via differential regulation of G3BP and TIA-1. *Hum. Mol. Genet.* **20**, 1400–1410.

Meyerowitz J., Parker S. J., Vella L. J. *et al.* (2011) C-Jun N-terminal kinase controls TDP-43 accumulation in stress granules induced by oxidative stress. *Mol. Neurodegener.* **6**, 57.

Namgung U. and Xia Z. (2000) Arsenite-induced apoptosis in cortical neurons is mediated by c-Jun N-terminal protein kinase 3 and p38 mitogen-activated protein kinase. *J. Neurosci.* **20**, 6442–6451.

Nelson R. J., Ziegelhoffer T., Nicolet C., Werner-Washburne M. and Craig E. A. (1992) The translation machinery and 70 kd heat shock protein cooperate in protein synthesis. *Cell* **71**, 97–105.

Neumann M., Sampathu D. M., Kwong L. K. *et al.* (2006) Ubiquitinated TDP-43 in frontotemporal lobar degeneration and amyotrophic lateral sclerosis. *Science* **314**, 130–133.

Ryabinina O. P., Subbian E. and Iordanov M. S. (2006) D-MEKK1, the Drosophila orthologue of mammalian MEKK4/MTK1, and Hemipterous/D-MKK7 mediate the activation of D-JNK by cadmium and arsenite in Schneider cells. *BMC Cell Biol.* **7**, 7.

Sreedharan J., Blair I. P., Tripathi V. B. *et al.* (2008) TDP-43 mutations in familial and sporadic amyotrophic lateral sclerosis. *Science* **319**, 1668–1672.

Stoecklin G., Stubbs T., Kedersha N., Wax S., Rigby W. F., Blackwell T. K. and Anderson P. (2004) MK2-induced tristetraprolin:14–3-3 complexes prevent stress granule association and ARE-mRNA decay. *EMBO J.* **23**, 1313–1324.

Udan M. and Baloh R. H. (2011) Implications of the prion-related Q/N domains in TDP-43 and FUS. *Prion* **5**, 1–5.

Vance C., Rogelj B., Hortobagyi T. *et al.* (2009) Mutations in FUS, an RNA processing protein, cause familial amyotrophic lateral sclerosis type 6. *Science* **323**, 1208–1211.

Xu Z. S. (2012) Does a loss of TDP-43 function cause neurodegeneration? *Mol. Neurodegener.* **7**, 27.

Zhang Y. J., Xu Y. F., Dickey C. A., Buratti E., Baralle F., Bailey R., Pickering-Brown S., Dickson D. and Petrucelli L. (2007) Progranulin mediates caspase-dependent cleavage of TAR DNA binding protein-43. *J. Neurosci.* **27**, 10530–10534.

NEUROPATHOLOGY

Neuropathology 2014; **34**, 45–48 doi:10.1111/neup.12046

Case Report

Cryptococcal meningitis accompanying lymphocytic inflammation predominantly in cerebral deep white matter: A possible manifestation of immune reconstitution inflammatory syndrome

Hiroya Kuwahara,[1,3] Kuniaki Tsuchiya,[2] Zen Kobayashi,[1,2] Akira Inaba,[3] Haruhiko Akiyama[2] and Hidehiro Mizusawa[1]

[1]Department of Neurology and Neurological Science, Graduate School, Tokyo Medical and Dental University, [2]Department of Dementia and Higher Brain Function, Tokyo Metropolitan Institute of Medical Science, Tokyo and [3]Department of Neurology, Yokosuka Kyosai Hospital, Kanagawa, Japan

Cryptococcal meningitis is rarely complicated by immune-mediated leukoencephalopathy, but the precise pathomechanism is uncertain. A 72-year-old Japanese man treated with prednisolone for Sweet disease developed a subacute progression of meningitis, which was considered as neuro-Sweet disease. A treatment by methylprednisolone rapidly improved CSF findings with a remarkable decrease in lymphocyte numbers in the blood, but the patient's consciousness still worsened after the cessation of the treatment. The patient developed cryptococcal meningitis and MRI showed abnormal intensities predominantly in the cerebral deep white matter along with the recovery of lymphocyte numbers in the blood, which resulted in death. A postmortem examination of the brain revealed degenerative lesions, especially at the cerebral white matter and cortex adjacent to the leptomeninges abundantly infiltrated by *Cryptococcus neoformans*. In the affected cerebral deep white matter, perivascular infiltration of lymphocytes was prominent in coexistence with reactive astrocytes and vascular proliferation, but these findings were not observed in the subcortical and cortical lesions. *Cryptococcus neoformans* was not present within the brain parenchyma. This is the first report of a case suggesting that cryptococcal meningitis can accompany lymphocytic inflammation predominantly in cerebral deep white matter as a possible manifestation of immune reconstitution inflammatory syndrome.

Key words: cerebral deep white matter, corticosteroid, cryptococcal meningitis, immune reconstitution inflammatory syndrome, neuro-Sweet disease.

INTRODUCTION

Cryptococcal meningitis is one of the most frequent fungal infections of the CNS and may accompany infectious granulomas (cryptococcomas) within the brain parenchyma.[1] Immune-mediated leukoencephalopathy is a rare complication of cryptococcal meningitis,[2] but the precise pathomechanism is uncertain. Here we report an autopsy case of cryptococcal meningitis accompanying lymphocytic inflammation predominantly in cerebral deep white matter, which could be considered as a unique manifestation of immune reconstitution inflammatory syndrome (IRIS).

CLINICAL SUMMARY

A 72-year-old man presented with a slight fever and headache, followed by a subacute progression of consciousness disturbance. One year earlier, he had suffered from multiple erythemas in his lower extremities, which was diagnosed as Sweet disease by skin biopsy, and had been treated with prednisolone for 1 year; An initial dose of 50 mg/day gradually decreased to 12.5 mg/day. Twenty days

Correspondence: Hiroya Kuwahara, MD, PhD, Department of Neurology and Neurological Science, Graduate School, Tokyo Medical and Dental University, 1-5-45, Yushima, Bunkyo-ku, Tokyo 113-8519, Japan. Email: h-kuwahara.nuro@tmd.ac.jp

Received 27 December 2012; revised 18 April 2013 and accepted 19 April 2013; published online 20 May 2013.

Fig. 1 Clinical course including the findings of CSF and the number of lymphocytes in the blood.

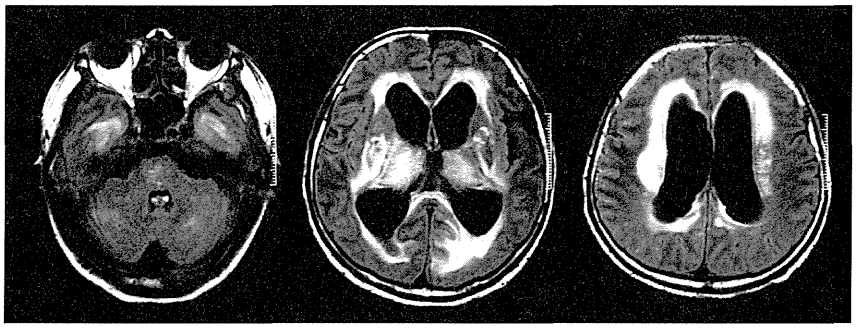

Fig. 2 Brain MRIs on day 35 showed hyperintensities in the cerebrum, cerebellum and brainstem on fluid-attenuated inversion recovery images; the cerebral deep white matter was most severely affected.

after the first symptom emerged, neurological findings were unremarkable except for drowsiness. Brain MRIs were normal, and CSF findings indicated meningitis (Fig. 1, day 20). There were no findings suggestive of infection or malignancy. HIV serology was negative. The patient was diagnosed as having possible neuro-Sweet disease (NSD) because HLA testing revealed HLA-Cw1, which has a strong association with NSD.[3] After we treated the patient with methylprednisolone 1 g/day for 3 days, the CSF findings rapidly improved with a remarkable decrease in the number of lymphocytes in the blood to 105/μL (Fig. 1, day 30). However, the patient's consciousness still worsened after the cessation of methylprednisolone. On day 35, brain MRI showed hyperintensities in the cerebrum, cerebellum and brainstem on fluid-attenuated inversion recovery images; the cerebral deep white matter was most severely affected (Fig. 2) and the lesions were partly enhanced by gadolinium. Along with the recovery of lymphocyte numbers in blood, the CSF demonstrated *Cryptococcus neoformans* with a decreased level of glucose (Fig. 1, day 36). Antifungal treatment using amphotericin B did not improve the patient's symptoms, and the patient died of respiratory failure on day 57 from the onset. Swelling of the superficial lymph nodes was not observed throughout the disease course. We considered that cryptococcal infection after treatment with methylprednisolone was fatal in our patient.

PATHOLOGICAL FINDINGS

A general autopsy was performed 9 h after the patient's death. There were no malignancies in visceral organs and no abnormalities in the lymph nodes. *C. neoformans* detected by Grocott and KB staining were accumulated at the leptomeninges of the brain and spinal cord (Fig. 3A,B). A striking finding was degenerative lesions in the cerebrum, cerebellum and pons. Notably, the degenerative lesions in the cerebrum were remarkable at the white matter and cortex adjacent to the leptomeninges, which were abundantly infiltrated by *C. neoformans*, especially near the frontal base, sylvian fissure and calcarine sulcus (Fig. 3C). In the affected deep white matter, perivascular infiltration of the lymphocytes was prominent (Fig. 3D), and reactive astrocytes and vascular proliferation were also evident. In contrast, vascular abnormalities and reactive astrocytes were not apparent in the subcortical and cortical lesions. Basal ganglia and thalamus were partly necrotic with slight infiltration of the lymphocytes. In the cerebellum, the subcortical white matter was extensively degenerated, but the deep white matter was mostly preserved (Fig. 3E). There were no apparent vascular abnormalities in the cerebellum. *C. neoformans* was not present within the parenchyma of the brain or spinal cord. There was no abnormal oligodendroglia suggestive of progressive multifocal leukoencephalopathy (PML), and JC virus was not detected in the cerebrum, cerebellum or brainstem by immunohistochemistry using an antibody against SV40.

DISCUSSION

IRIS is a condition observed mostly in immunocompromized patients, in which the immune system begins to recover and respond against a wide variety of pathogens with an overwhelming inflammatory response that

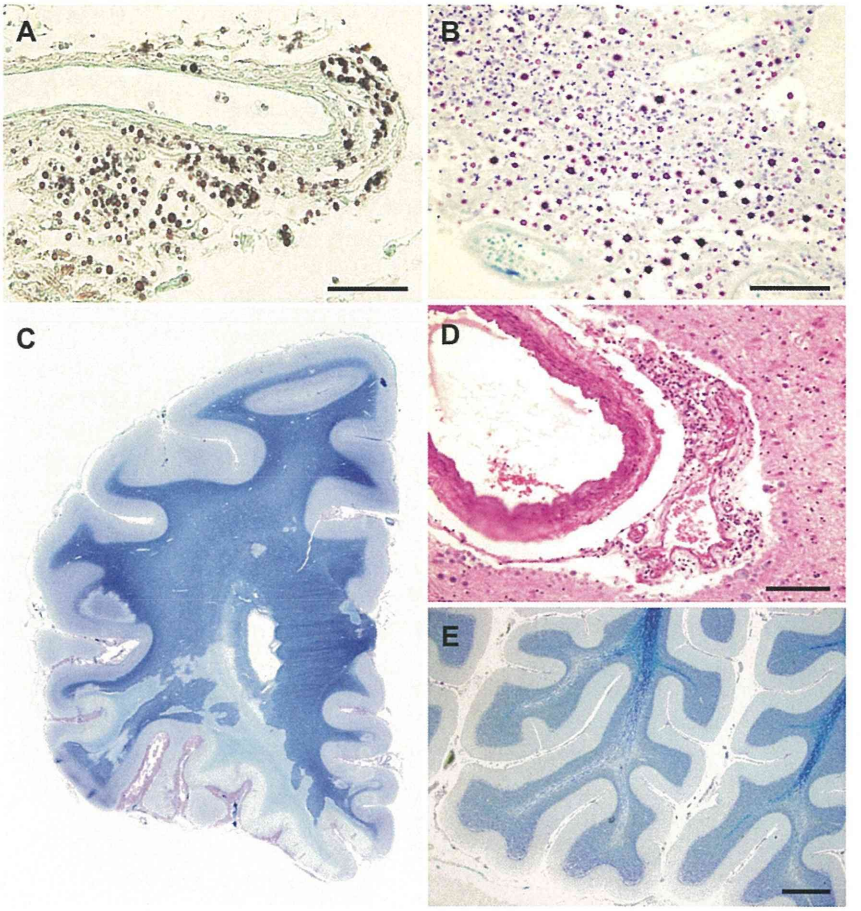

Fig. 3 (A, B) Grocott staining (A) and KB staining (B) showed *Cryptococcus neoformans* at the leptomeninges of the brain. Scale bar = 100 μm. (C) In the cerebrum, degenerative lesions were observed mainly at the white matter and cortex adjacent to the leptomeninges abundantly infiltrated by *C. neoformans*. (D) Perivascular infiltration of lymphocytes was evident in the cerebral deep white matter. Scale bar = 100 μm. (E) In the cerebellum, the subcortical white matter was extensively degenerated. Scale bar = 1 mm.

paradoxically makes the symptoms worse.[4] *C. neoformans* is a major pathogen associated with the occurrence of IRIS. IRIS is well recognized in HIV-infected patients receiving highly active antiretroviral therapy, but is also known as a complication of immunosuppressive treatment by corticosteroids.[5]

In our case, the pathology in the cerebral deep white matter indicated the pathomechanism of lymphocytic inflammation. Cryptococcal meningitis often accompanies lymphocytic infiltration within the brain parenchyma in the absence of *C. neoformans*,[1] but the degenerative changes of the cerebral white matter in the early phase of cryptococcal meningitis are mostly unremarkable. In our case, cryptococcal meningitis and the MRI abnormalities predominantly in the cerebral deep white matter occurred after the cessation of strong immunosuppressive treatment by methylprednisolone along with the recovery of lymphocyte numbers, and thus, the degenerative lesions in the cerebral deep white matter could be recognized as a manifestation of IRIS against an opportunistic infection of *C. neoformans* at the leptomeninges.

However, the degenerative lesions in the subcortical white matter and cortex were not accompanied by inflammation, and thus, the pathomechanism would be different from IRIS. The subcortical and cortical lesions, which were not manifested by MRI, were probably caused by disturbed cerebral hemodynamics which was frequently observed at the later stage of cryptococcal meningitis in HIV-negative adults.[6] In particular, the vascular inflammation in the cerebral deep white matter might contribute to the insufficiency of the blood flow to the cerebral subcortical white matter and cortex.

The pathomechanism of the lesions in the basal ganglia and thalamus might be IRIS because MRI abnormalities in these lesions were evident along with those in the cerebral deep white matter and the pathology involved inflammation. The pathomechanism of the cerebellar lesions was difficult to identify; there were no apparent findings of inflammation or PML.

Cryptococcal IRIS mainly manifests as lymphadenitis.[7] While cerebellitis has been reported as a manifestation of cryptococcal IRIS in the CNS,[8] pathological confirmation was absent. Thus, our case would be the first case of possible cryptococcal IRIS occurring in the brain which could be pathologically verified. The presence of the brain lesions and the absence of lymphadenitis in our case might be due

to some immunological host factor of the patient, including HLA.

Perivascular cuffing was also observed in an autopsy case of NSD.[9] Brain MRI before the treatment with methylprednisolone was normal in our case, and systemic corticosteroids are highly effective for most of the neurological manifestations in NSD patients.[3] Therefore, the brain pathologies in our case were unlikely as manifestation of NSD.

In conclusion, our autopsy case suggests that cryptococcal meningitis can accompany lymphocytic inflammation predominantly in cerebral deep white matter as a manifestation of IRIS.

REFERENCES

1. Lee SC, Dickson DW, Casadevall A. Pathology of cryptococcal meningoencephalitis: analysis of 27 patients with pathogenetic implications. *Hum Pathol* 1996; **27**: 839–847.
2. Wilcox RA, Thyagarajan D, Kempster P. Two cases of Cryptococcus meningitis presenting as leukoencephalopathy prior to amphotericin therapy. *Eur J Neurol* 2007; **14**: 350–352.
3. Hisanaga K, Iwasaki Y, Itoyama Y, Neuro-Sweet Disease Study Group. Neuro-Sweet disease: clinical manifestations and criteria for diagnosis. *Neurology* 2005; **64**: 1756–1761.
4. Shelburne SA, Montes M, Hamill RJ. Immune reconstitution inflammatory syndrome: more answers, more questions. *J Antimicrob Chemother* 2006; **57**: 167–170.
5. Gupta AO, Singh N. Immune reconstitution syndrome and fungal infections. *Curr Opin Infect Dis* 2011; **24**: 527–533.
6. Chang WN, Lu CH, Chang HW *et al.* Time course of cerebral hemodynamics in cryptococcal meningitis in HIV-negative adults. *Eur J Neurol* 2007; **14**: 770–776.
7. Skiest DJ, Hester LJ, Hardy RD. Cryptococcal immune reconstitution inflammatory syndrome: report of four cases in three patients and review of the literature. *J Infect* 2005; **51**: e289–e297.
8. Venkataramana A, Pardo CA, McArthur JC *et al.* Immune reconstitution inflammatory syndrome in the CNS of HIV-infected patients. *Neurology* 2006; **67**: 383–388.
9. Kokubo Y, Kuzuhara S, Isoda K, Sato K, Kawada N, Narita Y. Neuro-Sweet disease: report of the first autopsy case. *J Neurol Neurosurg Psychiatry* 2007; **78**: 997–1000.

Neuropathology and Applied Neurobiology (2013), **39**, 580–584 doi: 10.1111/nan.12022

Scientific correspondence

Transportin 1 accumulates in FUS inclusions in adult-onset ALS without *FUS* mutation

Accumulation of a protein, DNA/RNA binding protein fused in sarcoma (FUS), as cytoplasmic inclusions in neurones and glial cells in the central nervous system (CNS) is the pathological hallmark of amyotrophic lateral sclerosis (ALS) with *FUS* mutations (ALS-*FUS*) [1,2] as well as certain subtypes of frontotemporal lobar degeneration (FTLD-FUS) [3,4], the latter being unassociated with *FUS* mutations. While the inclusions in ALS-*FUS* contain only FUS, those in FTLD-FUS show co-accumulation of three proteins of the FET protein family, i.e. in addition to FUS, Ewing's sarcoma (EWS) and TATA-binding protein-associated factor 15 (TAF15) [5]. These findings strongly suggest that a more complex derangement of transportin-mediated nuclear import of proteins accounts for the disease process in FTLD-FUS in comparison to ALS-*FUS*. Recently, Neumann *et al.* reported that the inclusions in FTLD-FUS subtypes were strongly labelled for transportin 1 (TRN1) and that, as expected, the inclusions in ALS-*FUS* were completely unreactive for this protein [6].

Here we report an adult patient who exhibited a clinically pure ALS phenotype without *FUS* mutations (ALS-FUS) and cytoplasmic inclusions showing co-accumulation of FET and TRN1 proteins, confirming that ALS-FUS and FTLD-FUS represent part of a spectrum of FUS proteinopathy without *FUS* mutation.

A 65-year-old Japanese woman became aware of muscle weakness in her hands. Three years later, she was diagnosed as having ALS. Thereafter, bulbar palsy and respiratory distress progressed gradually; at the age of 70 years, tracheotomy and respirator support became necessary. The patient died of gastrointestinal bleeding at the age of 74 years, about 9 years after disease onset. There was no family history of neurological disorders, including ALS. During the disease course, dementia was not evident. We sequenced and found no mutations in the all coding regions of the *FUS* gene.

The brain was small and weighed 820 g (brainstem and cerebellum, 110 g) before fixation. The spinal cord showed marked atrophy. Histologically, loss of myelinated fibres was observed in the spinal white matter except for the posterior columns; the lateral corticospinal tracts appeared to be only mildly affected (Figure 1**a**). Neuronal loss and gliosis were also evident in the spinal anterior horns (Figure 1**b**) and brainstem hypoglossal nucleus. The presence of slightly basophilic round inclusions in the remaining lower motor neurones was a feature (Figure 1**c**). No Bunina bodies were found. In the cerebral cortex, mild neuronal loss was noted in the motor cortex. Immunostaining with an antibody against FUS (polyclonal, Sigma-Aldrich, St Louis, USA; 1:50) revealed widely distributed positive neuronal cytoplasmic inclusions (NCIs) in the CNS, including the spinal anterior horn and motor cortex (Figure 1**d**,**e**). The distribution and severity of FUS lesions and neuronal loss are shown in Table 1. FUS immunostaining also revealed positive glial cytoplasmic inclusions (GCIs) (Figure 1**f**). These cytoplasmic inclusions were also labelled by anti-ubiquitin (polyclonal, Dako, Glostrup, Denmark; 1:800) (Figure 1**g**) and anti-p62 (monoclonal; BD Bioscience, San Jose, CA, USA; 1:1000) antibodies (Figure 1**h**). No neuronal nuclear inclusions (NIIs) were found. The results of immunostaining for α-internexin and TDP-43 were all negative (data not shown).

Immunostaining with an antibody against transportin 1 (TRN1) (monoclonal, Abcam, Cambridge, UK; 1:200) also revealed clearly positive NCIs (Figure 2**a**) and GCIs. Such inclusions were also labelled with anti-TAF15 (polyclonal, Bethyl Lab, Montgomery, USA; 1:200) (Figure 2**b**) and anti-EWS (monoclonal, Santa Cruz, Santa Cruz, USA; 1:200) antibodies (Figure 2**c**). TRN1 and FUS were sometimes fully or partially colocalized in the same neurones (Figure 2**d**–**f**,**g**–**i**) and glial cells. The ratio of the colocalization (TRN1/FUS) in NCIs was about 50%.

FTLD-FUS can be classified into three pathological subtypes, atypical FTLD-U, neuronal intermediate filament inclusion disease (NIFID), and basophilic inclusion body disease (BIBD) on the basis of the morphology and distribution pattern of FUS-positive NCIs and NIIs [3]. Atypical FTLD-U is characterized by compact, round to oval kidney-shaped NCIs and vermiform NIIs in the neocortex, granule cells of the dentate gyrus, striatum and some other brain regions. NIFID is characterized by FUS-positive NCIs and NIIs as well as less predominant type IV interfilament-, α-internexin- and neurofilament-positive NCIs. Lastly,

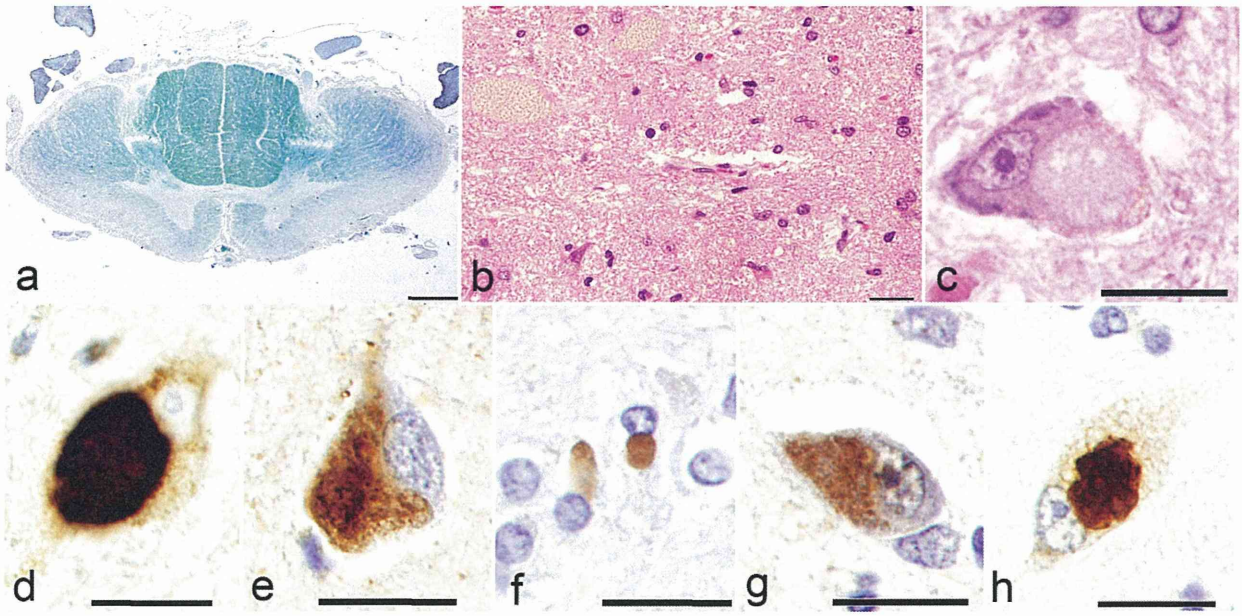

Figure 1. Light micrographs of nervous tissues from the patient. (**a**) A transverse section of the cervical cord (C7). Although mild, loss of myelinated fibres is evident in the bilateral lateral corticospinal tract regions. (**b**) Severe neuronal loss is evident in the cervical anterior horn (C7). (**c**) A light, slightly basophilic round inclusion is seen in the cytoplasm of a remaining anterior horn cell. (**d**,**e**) FUS-positive cytoplasmic inclusions are evident in a spinal anterior horn cell (**d**) and a motor cortex pyramidal neurone (**e**). (**f**) FUS-positive cytoplasmic inclusions are evident in two glial cells (oligodendrocytes) in the transverse fibres of the pons. (**g**,**h**) Such neuronal cytoplasmic inclusions are also positive for ubiquitin (**g**, oculomotor nucleus) and p62 (**h**, oculomotor nucleus). (**a**) Klüver–Barrera stain; (**b**,**c**) haematoxylin-eosin; (**d**–**f**) FUS immunostain; (**g**) ubiquitin immunostain; (**f**) p62 immunostain. Bars: (**a**) 1 mm, (**b**–**h**) 20 μm.

BIBD [7], in which basophilic NCIs stained with haematoxylin-eosin can be found in the affected regions, is characterized by widespread round or granular NCIs and few NIIs positive for FUS. It has been recognized that a clinically pure ALS phenotype, including the adult-onset disease, is present in BIBD [8,9]. Neumann *et al.* also included two cases of BIBD showing pure ALS phenotype [10,11] in their study (supplementary material) [6]; however, these cases were not fully examined genetically. The present case is a good example of the adult-onset, pure ALS phenotype of BIBD, with widespread FUS-positive NCIs and no NIIs in the CNS (Table 1). It is important to note that patients with the adult-onset ALS phenotype have so far been reported from only Japan [8–11].

In ALS-*FUS*, many of the reported mutations are present within the nuclear localization signal of the *FUS* gene, and the patients show only accumulation of FUS protein [12]. TRN1 is predominantly involved in the import of a number of heterologous ribonucleoproteins (hn-RNPs)-RNA binding proteins, including FUS. FUS-positive inclusions are strongly labelled for TRN1 in patients with FTLD-FUS, whereas in sharp contrast, such inclusions in those with ALS-*FUS* are not [6]. Therefore, it is possible to consider that aggregation of TRN1 is a significant event in the disease process in FTLD-FUS. It has been reported that almost all FUS inclusions in aFTLD-U (100%) and NIFID (99.4%) contained TRN1 [13]. Interestingly, in the present case, considerably fewer FUS inclusions contained TRN1.

In TDP-43 proteinopathy without *TDP-43* mutation, ALS is much more common than FTLD-TDP, although both diseases are recognized to represent part of a continuous spectrum [14]. In contrast, FTLD-FUS is the main phenotype in FUS proteinopathy without *FUS* mutation. In the present study, it was confirmed that – as is the case in sporadic TDP-43 proteinopathy – clinically pure ALS (ALS-FUS) exists as part of the sporadic FUS proteinopathy. Finally, ALS without *FUS* mutation (ALS-FUS) (also classified into BIBD) can be distinguished from ALS with *FUS* mutation (ALS-*FUS*) by neuropathological examination using TRN1 immunohistochemistry.

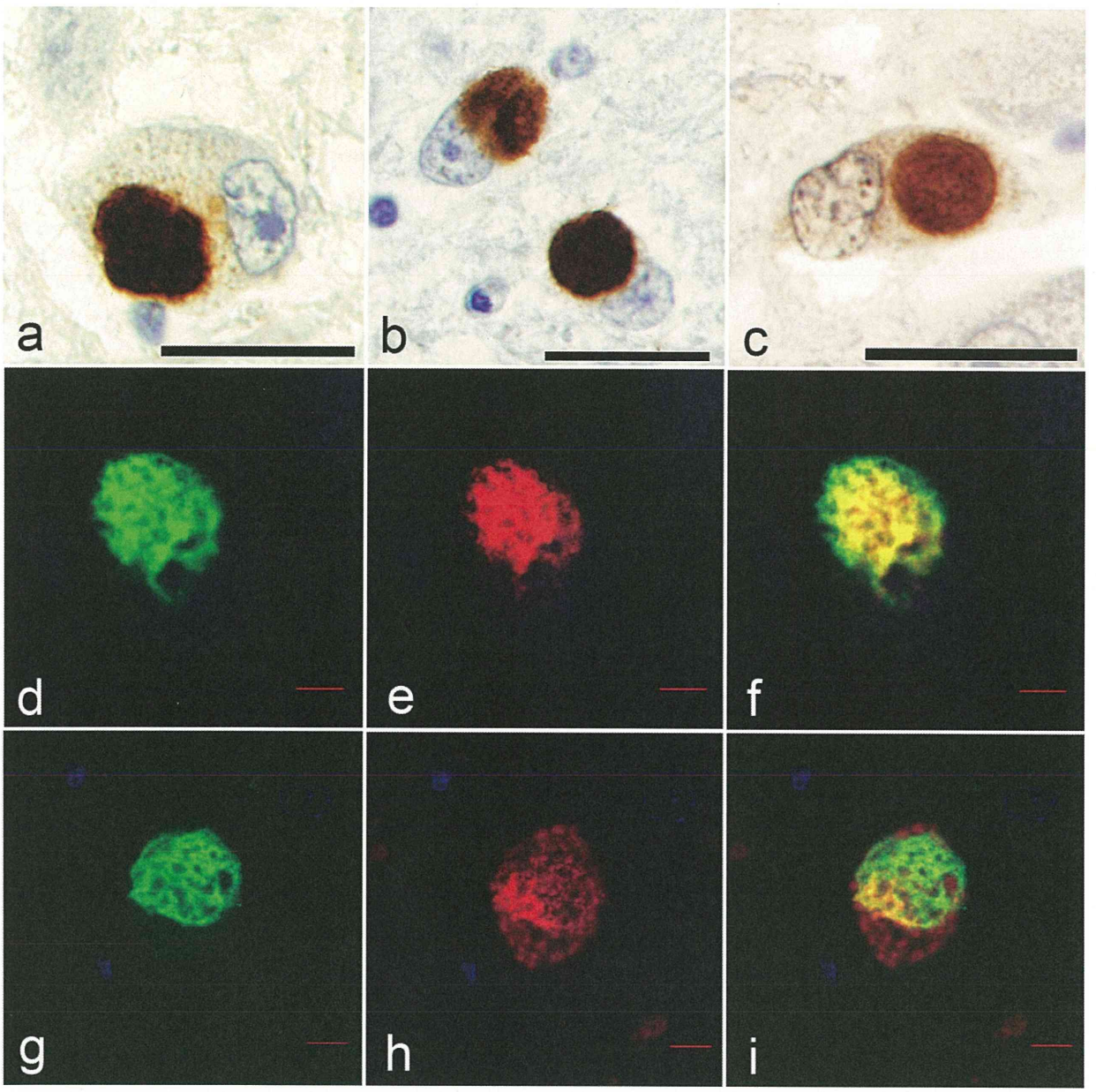

Figure 2. Immunohistochemistry using TRN1 and FET proteins. (**a–c**) Morphologically similar cytoplasmic inclusions are clearly labelled with anti-TRN1 (**a**, hypoglossal nucleus), anti-TAF15 (**b**, oculomotor nucleus) and anti-EWS (**c**, oculomotor nucleus) antibodies. (**d–i**) Double-labelling immunofluorescence, showing colocalization of FUS (green) and TRN1 (red) in a motor neurone of the lumbar anterior horn (**d–f**), and an inferior olivary nucleus neurone (**g–i**). Bars: (**a–c**) 20 μm, (**d–i**) 5 μm.

Acknowledgements

This work was supported by Grants-in-Aid, 23590390 (to Y.T.), and 20240037 and 23240049 (to H.T.), for Scientific Research from the Ministry of Education, Culture, Sports, Science, and Technology, Japan.

Author contributions

R.T., Y.T. and H.T. managed the study and were principally responsible for writing. R.T., Y.T., M.T., A.K. and H.T. performed the neuropathological observation and evaluation, R.T. and A.S. performed the sequencing analysis,

Table 1. Distribution and severity of FUS neuronal lesion and neuronal loss in the central nervous system

	Cerebral cortex	*Hippocampus*	*Striatum*	*Globus pallidus*	*Thalamus*	*Substantia nigra*	*Pontine nuclei*	*Inferior olivary nucleus*	*Vagus*	*CN XII*	*Cerebellar dentate*	*Spinal cord*
FUS pathology	+	–	+	++	++	++	+++	+++	–	+++	+++	+++
loss of neurones	+ (motor)	–	–	–	+	+	–	–	–	++	–	++

The presence and severity of neurone loss are represented as: – = not noted; + = minimal/mild; ++ = moderate/severe. Neurones containing FUS-positive inclusions were counted per 100 neurones in high-power fields, and the ratio is represented as: – = none; + = ~30%; ++ = 30~50%; +++ = ≧50%.

H.T., M.S. and M.N. examined the patient and carried out the clinical analysis, and K.K. and T.M. performed a general autopsy.

Conflict of interest

The authors declare that they have no conflict of interest.

R. Takeuchi*†
Y. Toyoshima*
M. Tada*
A. Shiga*
H. Tanaka‡
M. Shimohata‡
K. Kimura§
T. Morita§
A. Kakita*
M. Nishizawa†
H. Takahashi*

*Departments of *Pathology and †Neurology, Brain Research Institute, University of Niigata, and Departments of ‡Neurology and §Pathology, Shinrakuen Hospital, Niigata, Japan*

References

1 Kwiatkowski TJ Jr, Bosco DA, Leclerc AL, Tamrazian E, Vanderburg CR, Russ C, Davis A, Gilchrist J, Kasarskis EJ, Munsat T, Valdmanis P, Rouleau GA, Hosler BA, Cortelli P, de Jong PJ, Yoshinaga Y, Haines JL, Pericak-Vance MA, Yan J, Ticozzi N, Siddique T, McKenna-Yasek D, Sapp PC, Horvitz HR, Landers JE, Brown RH Jr. Mutations in the FUS/TLS gene on chromosome 16 cause familial amyotrophic lateral sclerosis. *Science* 2009; **323**: 1205–8

2 Vance C, Rogelj B, Hortobágyi T, De Vos KJ, Nishimura AL, Sreedharan J, Hu X, Smith B, Ruddy D, Wright P, Ganesalingam J, Williams KL, Tripathi V, Al-Saraj S, Al-Chalabi A, Leigh PN, Blair IP, Nicholson G, de Belleroche J, Gallo JM, Miller CC, Shaw CE. Mutations in FUS, an RNA processing protein, cause familial amyotrophic lateral sclerosis type 6. *Science* 2009; **323**: 1208–11

3 Mackenzie IR, Munoz DG, Kusaka H, Yokota O, Ishihara K, Roeber S, Kretzschmar HA, Cairns NJ, Neumann M. Distinct pathological subtypes of FTLD-FUS. *Acta Neuropathol* 2011; **121**: 207–18

4 Neumann M, Rademakers R, Roeber S, Baker M, Kretzschmar HA, Mackenzie IR. A new subtype of frontotemporal lobar degeneration with FUS pathology. *Brain* 2009; **132**: 2922–31

5 Neumann M, Bentmann E, Dormann D, Jawaid A, DeJesus-Hernandez M, Ansorge O, Roeber S, Kretzschmar HA, Munoz DG, Kusaka H, Yokota O, Ang LC, Bilbao J, Rademakers R, Haass C, Mackenzie IR. FET proteins TAF15 and EWS are selective markers that distinguish